Investigation of the Field Induced Antiferromagnetic Phase Transition in the Frustrated Magnet: Gadolinium Gallium Garnet

P. Schiffer, A. P. Ramirez, D. A. Huse, and A. J. Valentino
AT&T Bell Laboratories, Murray Hill, New Jersey 07974
(Received 20 May 1994)

The geometrically frustrated magnet gadolinium gallium garnet (GGG) has a unique low temperature (<0.38 K) antiferromagnetic phase which exists only in finite fields ($H \sim 1$ T). We have measured the specific heat and magnetic susceptibility of GGG to obtain the first accurate map of the low temperature phase diagram. A ground state magnetic structure in this field regime has been determined by simulations including both the exchange and dipole interactions. We find a critical exponent $\alpha < 0$ at the ordering transition, consistent with a transition in a random magnetic environment.

PACS numbers: 75.30.Kz, 75.40.Gb

There has been much recent interest in magnetic materials which exhibit strong antiferromagnetic tendencies but which are prevented from ordering at temperatures near the exchange energy by uniform geometric frustration of the spins [1]. One such material is $Gd_3Ga_5O_{12}$ (gadolinium gallium garnet or GGG), in which the magnetic Gd ions are on two interpenetrating corner-sharing triangular sublattices within the garnet structure, and the exchanges are almost purely antiferromagnetic (AFM) with $\Theta_{Weiss} \sim -2$ K [2,3]. GGG has long been used in magnetic bubble memories and can thus be obtained in single crystals of exceptional purity and very low disorder. The availability of high quality GGG samples and the depth to which the high temperature (>0.5 K) properties are understood make it a model system for the study of frustrated magnets.

Because of the high degree of frustration, long-range AFM order is suppressed in GGG to $T \ll \Theta_{Weiss}$ and appears to be completely suppressed in low magnetic fields [4–6]. A brief report [5] of magnetic susceptibility (χ) measurements at low temperatures indicated an AFM ordering transition as the external magnetic field was increased to ~1 T and a return to paramagnetism at a somewhat higher field. Specific heat (C) and thermal expansion measurements [7] confirmed the existence of a transition, although the phase boundaries varied widely between measurements. Neutron scattering experiments have not been attempted, due to the high absorption of neutrons by ^{157}Gd nuclei.

In this Letter we present new measurements of C and χ which allow a detailed study of this unique low temperature field-induced antiferromagnetism, including the first accurate map of the phase diagram for GGG. The ground state magnetic structures in both the AFM and paramagnetic (PM) phases are determined from simulations which include both the AFM exchanges and the considerable dipole interaction. Measurements of the critical behavior of both C and χ at the ordering transition yield a critical exponent $\alpha < 0$, which is consistent with a transition in a random magnetic environment.

The magnetic Gd ions in GGG are on two equivalent sublattices of corner sharing equilateral triangles [8]. The Gd spins ($S = 7/2$) are isotropic, although there is a small single ion anisotropy in the gadolinium garnets of less than 0.04 K [9]. This isotropy leads to the high degree of frustration in GGG which prevents ordering at low fields of the sort observed in isomorphic magnetic garnets such as $Dy_3Al_5O_{12}$ (DAG). The nearest neighbor dipole energy is ~0.7 K, and the nearest neighbor exchange energy is $J_{NN}S(S+1) \cong 1.5$ K. Further neighbor exchanges are known to be an order of magnitude or more smaller from previous high temperature measurements [2].

We have measured χ and C on two samples of GGG cut from the same single crystal grown by the Czochralski method. Both samples had a needlelike shape (with aspect ratios of ~5 and ~20, respectively), and the needle axis and the external magnetic field were along the [100] direction (the qualitative features of the phase diagram seem to be independent of field orientation [5,7]). The level of crystalline imperfections in GGG crystals grown by this technique is extremely small [4,10,11]; the only significant defect is an off stoichiometry of ~1% additional Gd ions sitting on Ga sites which is inherent in the crystal growth process. The measurement techniques for both χ and C have been described previously [4].

In Fig. 1 we display typical measurements of χ as a function of field. At high temperature, χ decreases monotonically with H as the Zeeman energy suppresses spin fluctuations [6]. As the sample is cooled, a broad peak appears in $\chi(H)$ corresponding to the quenching of AFM short range order (SRO) by the field. Below ~0.38 K, two increasingly sharp peaks appear on either side of this feature, corresponding to the transitions to and from long range order (LRO) as the field is increased. Both the LRO and SRO peaks are shown in Fig. 2; note that the LRO peaks in Fig. 1 become sharper at lower temperature due to the isotherm being more normal to the phase boundary. The inset to Fig. 1 shows an enlargement of $\chi(H)$ in the ordered phase at low temperatures: In addition to the two LRO peaks there is a

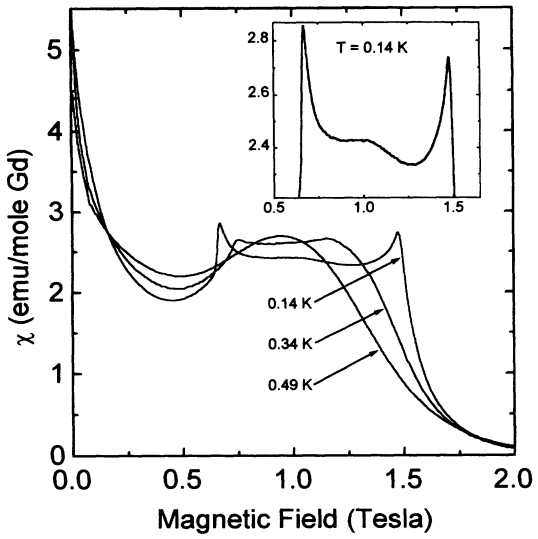

FIG. 1. The magnetic susceptibility of GGG at several temperatures. Inset shows an enlargement at $T = 0.14$ K, note the broad peak in the center of the ordered phase.

broad bump in the center of the phase, a previously unseen feature.

In Fig. 3, we show measurements of C as a function of temperature at several fields. A broad peak at low fields and high temperatures corresponds to the formation of AFM SRO which is quenched at high fields. Again the sharpness of the LRO peak depends on the angle at which the data isochore intersects the phase boundary. The entropy obtained by integrating C/T across the LRO peak is only a small fraction of the total magnetic entropy. This indicates that much of the ordering takes place at higher temperatures which is consistent with the observed SRO peaks.

The phase boundary of the AFM phase given by the LRO peaks in Fig. 3 was not obtained directly from the peak positions, since the relevant field is not the external magnetic field H_{ex}, but the internal field given by $H_i = H_{ex} - 4\pi NM$, where M is the magnetization (obtained by integrating χ) and N is the demagnetization factor determined by the sample geometry [12]. The correction was not made in the previous preliminary [5,7] studies of the phase diagram, since the values of M were not available. This accounts for the significant discrepancies between their phase diagrams and also for their phase boundaries being at higher fields than those given here. For our needlelike samples, N was easily calculable [12] and $4\pi NM$ was typically ~50 mT for the χ sample and ~5 mT for the C sample. The excellent agreement between the two measurements indicates that we are measuring the true phase boundary.

The AFM phase in GGG exists when the Zeeman energies associated with the external field are of the same order as the AFM exchange energy. A field of that magnitude alleviates the local geometric frustration but does not force the magnetization to saturate. While some other materials [13] have similar phase diagrams, they are due to a field-induced change from an nonmagnetic singlet to a magnetic doublet state which is a single-ion effect rather than the inherently many-body frustration-induced behavior in GGG. One particularly interesting feature of the GGG phase boundary is the slight upward curvature of the low field boundary as $T \rightarrow 0$ which is also seen in the unpublished data of Ref. [5]. This temperature-reentrant behavior indicates that the AFM ordered phase has more entropy than the low temperature PM phase in that region, an unusual phenomenon that also occurs on the phase boundary between solid and liquid helium. This suggests that the "disordered" paramagnetic phase in that region

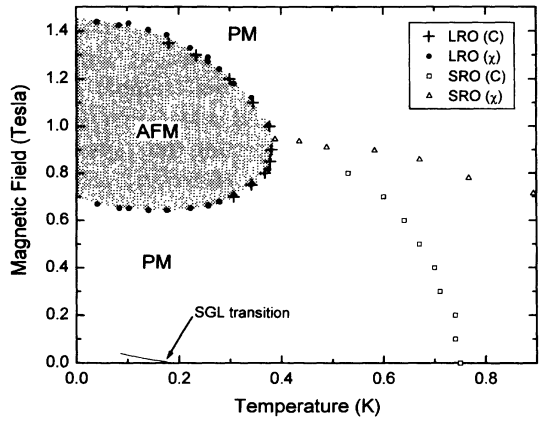

FIG. 2. The magnetic phase diagram of GGG. The long range order peaks which define the antiferromagnetic (AFM) phase boundary and the short range order peaks in the paramagnetic (PM) phase are shown. The line of maxima in χ vs T corresponding to the spin-glass-like freezing transition is also shown.

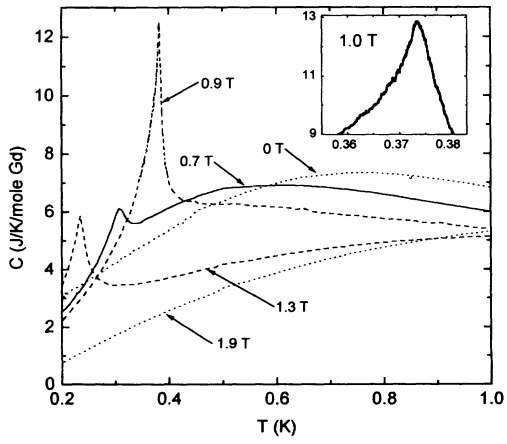

FIG. 3. The specific heat of GGG at several fields. The inset shows the critical behavior at 1.0 T.

actually possesses a high degree of magnetic order, even though there is no sharp ordering feature in the measured quantities.

To further understand magnetic ordering in GGG, we have studied a simple model consisting of classical Heisenberg spins at each Gd site coupled with nearest-neighbor isotropic antiferromagnetic exchange interactions and dipolar interactions to the third nearest neighbor. The nearest-neighbor exchange is assumed to be twice the strength of the nearest-neighbor dipolar interactions. We examined ground states as a function of field and also finite temperature behavior in Monte Carlo simulations. We have determined the PM spin configuration in the high temperature and the high field regimes, and we also have found a magnetically ordered phase with approximately the same boundary as seen experimentally.

The nature of the ordering found in this model is illustrated in Fig. 4, which shows the 24 Gd sites in a cubic unit cell of GGG projected along the z axis. The structure does not have inversion symmetry but is invariant under 180° rotations about certain symmetry axes. The sites at the edges and at the center of Fig. 4 ("A" sites) are on twofold axes that run parallel to the z axis, so when the applied field is also along the z axis (as in our experiment) these sites are of higher symmetry than the others ("B" sites).

In the PM phase at fields above the upper critical field or at temperatures above the transition, the local magnetization at the A sites points along the field direction (the z axis). At the B sites, due to the dipolar interactions and the lower symmetry, the local magnetizations in the PM phase have components along either the x or y axis as shown by the dashed arrows in Fig. 4. The vanishing of one Cartesian component of the local magnetization at each of the B sites when a field is applied along the z axis creates an Ising-like symmetry that is broken in the ordered phase. Calculations of $\chi(H)$ at temperatures above the ordering temperature reproduce the experimentally observed broad peak at fields corresponding to ~1 T. In the model this peak is due to the A spins flipping to align parallel to **H** from their low field state of being antiparallel to **H** (due to AFM exchange with the more numerous B spins). Our calculations did not confirm that the above PM state describes GGG near $T = 0$ at fields below the lower critical field since there the model has many metastable states and long equilibration times. Considering the unusual upward curvature of the low field phase boundary, it would not be surprising if there were some more exotic magnetic behavior in that regime.

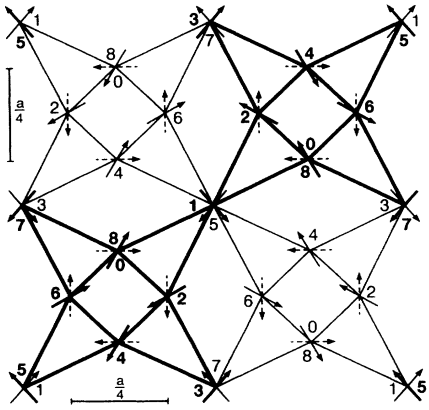

FIG. 4. The magnetic structure of GGG in the AFM and PM phases as described in the text. The projection of one unit cell along a [100] direction (z axis pointing out of the page) is shown with the heights of each site along the z axis shown in units of $a/8$, where a is the unit cell size. The arrows indicate the x-y components of the magnetizations. Dashed arrows are in the PM phase and solid are in the AFM phase.

In the model's ordered AFM phase, the local magnetizations at the A sites have components in the x-y plane as well as along the z axis (field direction), and the local magnetizations at the B sites rotate away from the x-z or y-z planes in which they point in the PM phase. The ordering is most simply described in terms of an Ising-like variable σ which corresponds to the direction (clockwise or counterclockwise) the x-y components ($\mathbf{m}_i$) of the local magnetizations point around each nearest-neighbor triangle when viewed down the z axis [$\sigma = \mathrm{sgn}(\mathbf{m}_i \times \mathbf{r}_i)$, where i is any spin in the triangle and $\mathbf{r}_i$ is the vector from the center of the triangle to that spin's lattice site projected onto the x-y plane]. These components are shown by the solid arrows in Fig. 4, with the two sublattices denoted by bold and fine symbols (note that each spin's nearest neighbors are all on the same sublattice). Triangles that share a corner always have opposite σ, thus there are two degenerate states for each sublattice and four equivalent ordered states for the system, one of which is shown in the figure.

The phase boundary we obtain from the simulations is uniformly ~30% outside the experimental boundary in both T and H which is consistent with quantum fluctuations or disorder in the real sample suppressing ordering. The lower critical field is least precisely located, due to the problems equilibrating the system in that regime as mentioned above. However, at low fields, we have found lower energy states than the ordered state of Fig. 4, showing that the lower critical field for that phase is indeed nonzero. Although we could not numerically reproduce the broad bump in $\chi(H)$ experimentally observed in the AFM phase, this is likely associated with the polarization of the A sites which also creates the broad SRO feature in $\chi(H)$ at high temperatures.

The high resolution with which we measured C and χ allowed us to analyze the critical behavior at the LRO transition, which is presumably affected by the large roles frustration and dipole forces play in shaping the phase boundary. We expect the same critical behavior in C and

χ since both quantities are second derivatives of the free energy with respect to the intensive quantity (temperature or field) which is being varied as the phase boundary is being crossed. In fact, the qualitative shapes of the LRO peaks in C and χ are quite similar in that both are much steeper on the PM sides of the transition. The rounding of the peaks (~2 mK for C and typically ~10 mT for χ) is consistent with demagnetization effects in the respective samples.

For the purposes of analysis, we assumed that the critical behavior at the transition could be described by $C^{\pm} = B + A^{\pm}t^{-\alpha}$ where $\pm$ indicates the behavior above and below T_c, B is the background specific heat which to lowest order is constant near T_c, and $t \equiv |T - T_c|/T_c$ is the reduced temperature. One can subtract the expressions above and below T_c from each other to obtain $\Delta C = |C^+ - C^-| = |A^+ - A^-|t^{-\alpha}$ which, when plotted vs t on a logarithmic scale, gives the critical exponent α. Typical data are shown in Fig. 5. Notice that the critical regime over which we obtain a good linear fit is approximately a decade in t. Unfortunately, α obtained by this method is very strongly dependent on the assumed value of T_c, and the few mK of rounding in our data prevents the precise determination of α. We obtain $\alpha = -0.7 \pm 0.35$ using only values of T_c which yield a good linear fit to the data over a decade in reduced temperature. By varying T_c further, however, we see linear behavior in ΔC over at least a half decade with $-1.2 < \alpha < -0.1$. Although the data in χ are limited by more rounding and a more limited range of critical behavior, they also yield $\alpha < 0$.

Models of critical behavior in which one expects $\alpha < 0$ include Heisenberg systems (such as Fe and Ni) and Ising systems with disorder (random exchanges or fields) [14]. The former is an unlikely model for GGG despite the isotropy of the individual Gd spins, since there is a great deal of anisotropy in the environment from the dipole interactions (although one similarity is the long range nature of both the RKKY interaction in Fe and Ni and the dipole interaction in GGG). Despite the highly site-ordered nature of the lattice, the transition might be described as Ising spins in a random environment since our simulations do predict an Ising-like symmetry in the PM phase. The randomness might be explained by the ~1% excess Gd ions which should be randomly placed and should therefore produce random exchange disorder as well as random fields due to their polarization by the applied field. Since we observed critical behavior in C from within $\sim 10^{-1.5}$–$10^{-2.5}$ of T_c, the correlation volume of the ordered state should include ~10 or more nearest neighbor spacings (assuming a typical critical exponent $\nu \geq \frac{2}{3}$) or at least $\sim 10^3$ spins. Thus all the spins should be correlated with the relatively sparse excess Gd ions.

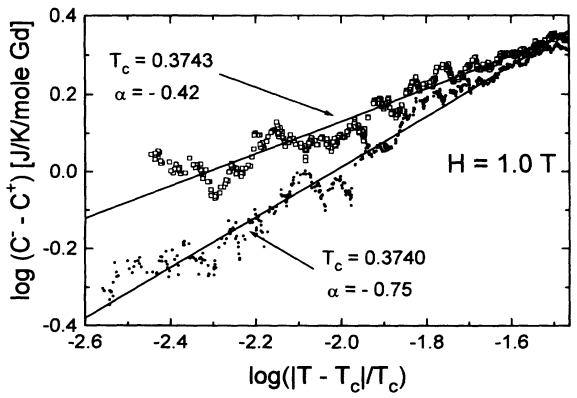

FIG. 5. The critical behavior in C at the boundary of the AFM phase at $H = 1.0$ T. Note the sensitivity of α to T_c.

In conclusion, we have made the first detailed study of the low temperature properties of GGG in a magnetic field. In addition to mapping the phase diagram, we have proposed a model for the magnetic structure and analyzed the critical behavior at the AFM ordering transition. Further experimental and theoretical efforts are certainly warranted in this model magnetic system with its unique combination of strong geometric frustration and dipolar interactions.

The authors are grateful for helpful discussions with G. Aeppli, C. Broholm, V. Fratello, and C. D. Brandle. We thank V. Fratello for sample preparation and A. Skjeltorp for sharing unpublished data with us.

[1] A. P. Ramirez, Annu. Rev. Mater. Sci. **24**, 453 (1994); R. Liebmann, *Statistical Mechanics of Periodic Frustrated Ising Systems* (Springer-Verlag, Berlin, 1986).
[2] W. I. Kinney and W. P. Wolf, J. Appl. Phys. **50**, 2115 (1979); W. I. Kinney, Ph.D. thesis, Yale University, 1979 (unpublished).
[3] W. P. Wolf *et al.*, J. Phys. Soc. Jpn (Supp. B1) **17**, 443 (1962).
[4] In fact a spin-glass-like transition has been observed for $H = 0$ at low temperatures. P. Schiffer *et al.* (unpublished).
[5] S. Hov, H. Bratsberg, and A. T. Skjeltorp, J. Magn. Magn. Mater. **15–18**, 455 (1980); S. Hov, Ph.D. thesis, University of Oslo, 1979 (unpublished).
[6] D. G. Onn, H. Meyer, and J. P. Remeika, Phys. Rev. **156**, 663 (1967); R. A. Fisher, G. E. Brodale, E. W. Hornung, and W. F. Giauque, J. Chem. Phys. **59**, 4652 (1973).
[7] A. P. Ramirez and R. N. Kleiman, J. Appl. Phys. **69**, 5252 (1991).
[8] See Fig. 1 in Ref. [4].
[9] J. Overmeyer *et al.*, *Paramagnetic Resonance* (Academic Press, New York, 1963).
[10] V. Fratello (private communication).
[11] B. Daudin, R. Lagnier, and B. Salce, J. Magn. Magn. Mater. **27**, 315 (1982).
[12] J. A. Osborn, Phys. Rev. **67**, 351 (1945).
[13] R. L. Carlin and L. J. De Jongh, Chem. Rev. **86**, 659 (1986).
[14] D. P. Belanger, Phase Transitions **11B**, 53 (1988), and references therein.

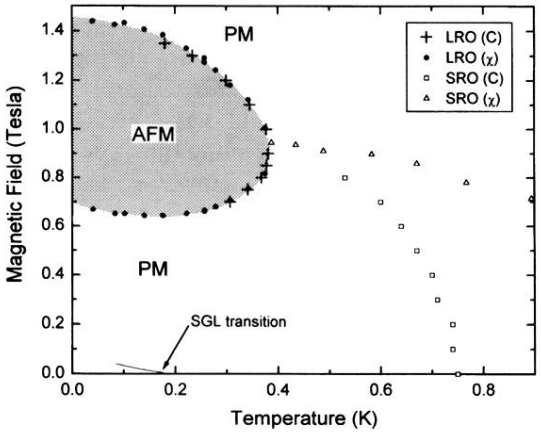

FIG. 2. The magnetic phase diagram of GGG. The long range order peaks which define the antiferromagnetic (AFM) phase boundary and the short range order peaks in the paramagnetic (PM) phase are shown. The line of maxima in χ vs T corresponding to the spin-glass-like freezing transition is also shown.